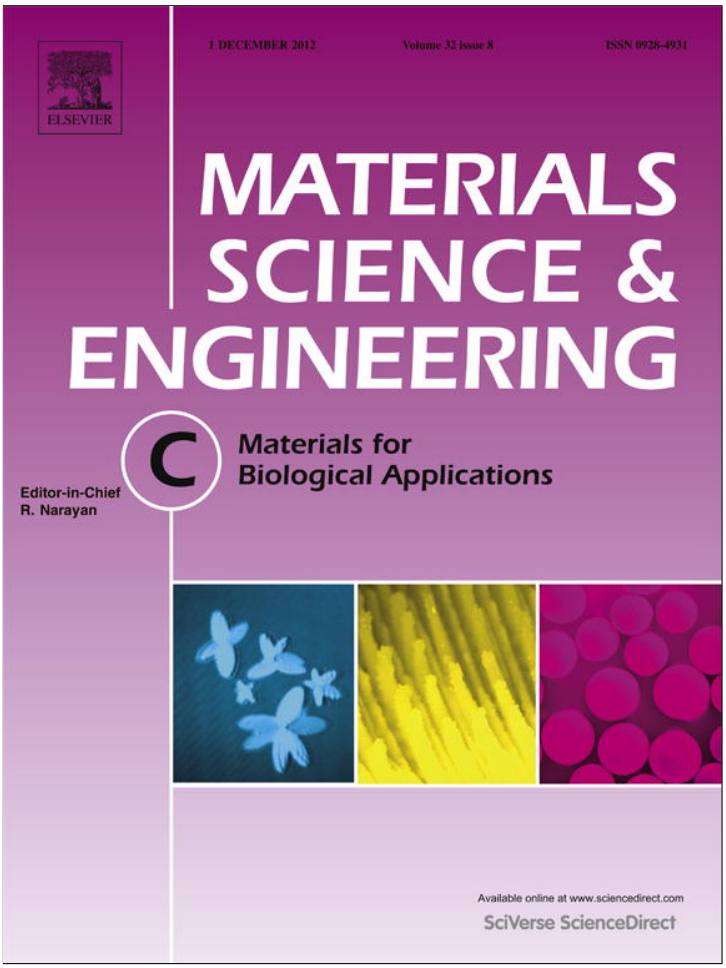

Materials Science and Engineering C 32 (2012) 2501–2507

Contents lists available at SciVerse ScienceDirect

Materials Science and Engineering C

journal homepage: www.elsevier.com/locate/msec

Effects of protein-simulated body fluid mixing methods on characteristics of bone-like mineral

Ho-Jun Song [a], Yeong-Joon Park [a], Won-Jin Moon [b], Linh N. Luong [c], David H. Kohn [c,d,*]

[a] Department of Dental Materials and MRC for Biomineralization Disorders, School of Dentistry, Chonnam National University, Gwangju 500–757, Korea
[b] Korea Basic Science Institute, Gwang-Ju Center, 300 Yongbong-dong, Book-gu, Gwangju 500–757, Korea
[c] Biomedical Engineering, University of Michigan, Ann Arbor, MI 48109-2110, USA
[d] Biologic & Materials Sciences, University of Michigan, Ann Arbor, MI 48109-1078, USA

ARTICLE INFO

Article history:
Received 20 January 2012
Received in revised form 19 June 2012
Accepted 20 July 2012
Available online 27 July 2012

Keywords:
Bone-like mineral
Poly(lactic-co-glycolic acid)
Bovine serum albumin
Simulated body fluid
Coprecipitation

ABSTRACT

This study examined effects of protein mixing methods into modified simulated body fluid (mSBF) on the crystalline structure and morphology of bone-like mineral (BLM) coated on a poly(lactic-co-glycolic acid) template (PLGA). Using bovine serum albumin (BSA) as a model protein, four sample groups were prepared: the N-BLM group was coated by soaking substrates in mSBF without BSA; the B-BLM group was coated by soaking in mSBF with BSA added immediately before soaking; the Ca-BLM group was coated by soaking in Ca-mSBF prepared by premixing BSA with a $CaCl_2$ solution before preparing the mSBF; the P-BLM group was coated by soaking in P-mSBF made by premixing the BSA with a KH_2PO_4 solution. The B-BLM and Ca-BLM groups exhibited densely coated, thick BLM layers, whereas the P-BLM group exhibited loosely connected BLM clusters. The hydroxyapatite (HAp) crystallites of the B-BLM and Ca-BLM groups were aligned along the c-axis, but those of the P-BLM group were disordered and had a lower crystallinity. The alignment to the c-axis of Ca-BLM and the disordered orientation of P-BLM were caused by calcium ions bound to BSA in Ca-mSBF and phosphate ions bound to BSA in P-mSBF, respectively. These results show that the crystallinity and morphology of BLM can be controlled by the mixing of BSA in mSBF. The crystallinity of BLM is closely connected to its solubility. Therefore, the release characteristics of growth factors and cell regulation on BLM could be affected by the changes in the crystalinity of BLM.

1. Introduction

Bone-like mineral (BLM) coatings on biomaterials, such as titanium alloys and biodegradable polymers, lead to improved bioactivity and osteoconductivity [1,2]. Osteoinductivity can be achieved by delivering biological factors to local sites, by binding the factors to biomaterials and by controlling their release [3,4]. Coprecipitation of BLM and growth factors, which is achieved by incubating a substrate in a simulated body fluid (SBF) containing growth factors, is one strategy for incorporating growth factors into BLM [5,6]. When growth factors are incorporated via coprecipitation, their biological activity remains high because the BLM is coated onto the substrate at physiological temperature, and the loading capacity of growth factors in BLM is higher than that achieved via adsorption [5,7]. In addition, the growth factors are incorporated through the thickness of the BLM by the coprecipitation method, and are released slowly, whereas growth factors adsorbed to a surface undergo only a burst release. The different release profiles also result from the fact that during coprecipitation, growth factors are chemically bound to the three-dimensional crystal lattice of the BLM vs. just weakly adsorbed [5].

The release characteristics of growth factors from BLM in-vitro and in-vivo depend on the rate of BLM dissolution and the chemical binding states between the growth factors and BLM. The dissolution rate of BLM is related to its crystalline structure. Therefore, it is important to determine how growth factors affect the crystalline structure of BLM and chemical binding state. Bovine serum albumin (BSA) has been used as a model protein in coprecipitation research. BSA inhibits BLM formation and decreases its crystallinity [5,8,9]. In contrast, Wen et al.[1] reported that BSA coprecipitation increases the crystallinity of BLM and coprecipitated BLM has a dominant HAp crystalline structure with a more preferred orientation to the c-axis compared to BLM without BSA. Therefore, the effect of proteins on the growth and crystal structure of BLM and the specific growth mechanisms are in need of further investigation if general rules for using BLM in drug delivery applications are to be defined. We hypothesize that the chemical interaction between BSA and inorganic ions in SBF affects the crystalline structure of BLM. The chemical interactions between proteins and ions in SBF can be modified by changing the BSA mixing procedure during the process of making SBF. In most studies investigating BSA/apatite coprecipitation, BSA has been simply mixed

* Corresponding author at: 1011 N. University Ave., Room 2213, Ann Arbor, MI 48109–1078. Tel.: +1 734 764 2206; fax: +1 734 647 2110.
E-mail address: dhkohn@umich.edu (D.H. Kohn).

0928-4931/$ – see front matter © 2012 Elsevier B.V. All rights reserved.
http://dx.doi.org/10.1016/j.msec.2012.07.032

into the pre-made SBF in [1,5–7,10]. Therefore, this study examined the effects of the BSA mixing procedure on the crystalline structure of BLM coprecipitated with BSA on PLGA substrates.

2. Materials and methods

Poly(lactic-co-glycolic acid) (PLGA) films were prepared using 20 wt% PLGA (85:15 PLA:PGA ratio, Sigma-Aldrich, lot no. MKBG8825V, USA) in a chloroform solution. The PLGA solution was poured over 18×18 mm^2 cover glasses, and air-dried for at least 24 h. The films were etched in 0.5 M NaOH for 15 min followed by ultrasonic rinsing in distilled water. A modified simulated body fluid (mSBF) [5,11], which contains 2× the concentration of Ca^{2+} and HPO_4^{2-} as standard SBF [12], was used to mineralize the films. mSBF contained the following reagents in ultrapure water (Millipore, Milli-Q, USA): 141 mM NaCl, 4.0 mM KCl, 0.5 mM $MgSO_4$, 1.0 mM $MgCl_2$, 4.2 mM $NaHCO_3$, 5.0 mM $CaCl_2\,2H_2O$, and 2.0 mM KH_2PO_4. mSBF was titrated to pH 6.8 using NaOH.

The BLM coating was deposited onto PLGA films by soaking the films in mSBF. The non-coprecipitated bone-like mineral control group (N-BLM) was prepared using mSBF without BSA. To fabricate the BSA-coprecipitated samples (B-BLM), BSA (BioShop, lot no. 9D11406, Canada) was added to mSBF immediately before soaking the specimens, which is designated B-mSBF. An additional two groups were prepared to investigate the effect of the BSA mixing methods with mSBF on the characteristics of BLM. BSA was premixed with a $CaCl_2$ solution before preparing mSBF, and then kept at 37 °C for 24 h. This solution was used instead of $CaCl_2$ while preparing the mSBF. The Ca-BLM group was fabricated using this variant of mSBF, which is designated Ca-mSBF. The P-BLM group was fabricated using a P-mSBF prepared by premixing BSA with a KH_2PO_4 solution and applying similar procedures to that used for Ca-mSBF. The pH of the BSA-containing $CaCl_2$ and KH_2PO_4 solutions were 6.0 and 5.6, respectively. The BSA concentration in mSBF was 200 μg/ml for all groups. All specimens were soaked in 15 ml of mSBF for 6 days at 37 °C. The solutions were exchanged daily to replenish the ion concentration to the supersaturated levels. For the B-BLM group, new BSA was added to mSBF immediately before soaking the specimens. Four specimens from each group used for each measurement.

Cross-sectional images of the sample groups were observed by field emission scanning electron microscopy (FE-SEM; Hitachi S-4700, Japan). BSA incorporation into BLM was examined by FT-IR spectroscopy (Spectrum 400, PerkinElmer, UK) with an attenuated total reflectance (ATR) accessory. The crystalline structure was analyzed by X-ray diffraction (XRD; PANalytical, X'Pert PRO, Netherlands) with Cu Kα radiation (30 mA, 40 kV) at a scan speed of 0.067°/s from 10° to 80°. The intensities and the values of full width half maximum (FWHM) of XRD peaks were analyzed by ANOVA with Tukey post-hoc tests to determine the effects of mixing method. The morphology and structure of the crystallites were examined by high resolution transmission electron microscopy (HRTEM; Techni F20, Philips, Netherlands) operating at 200 kV. The TEM specimens were prepared by cutting the BLM films coated on PLGA in cross-sectional direction using a focused ion beam (FIB; FEI Co., Quanta 3D, Netherlands). Therefore, the cross-sectional plane of each BLM film, perpendicular to the BLM growth direction, was analyzed by TEM. The chemical binding states were analyzed by X-ray photoelectron spectroscopy (XPS; Multilab 2000, VG, UK). The XPS spectra were obtained for all groups and BSA powder using monochromatic Al Kα radiation with a take-off angle of 90°. High-resolution narrow scanning was performed for the C 1 s, N 1 s, Ca 2p and P 2p peaks.

3. Results and discussion

BLM layers were coated onto the PLGA substrates, and BLM clusters were grown on the initial BLM layers (Fig. 1). Large-sized BLM clusters aggregated with 10–20 m sized particles were observed on BLM layers of approximately 3 μm thickness for the N-BLM group. Thicker BLM layers of 5–6 μm thickness were grown under the B-mSBF and Ca-mSBF conditions, with BLM clusters grown on Ca-BLM, but not B-BLM. The BLM clusters were grown in a disordered manner on a thinner BLM layer of 1 μm

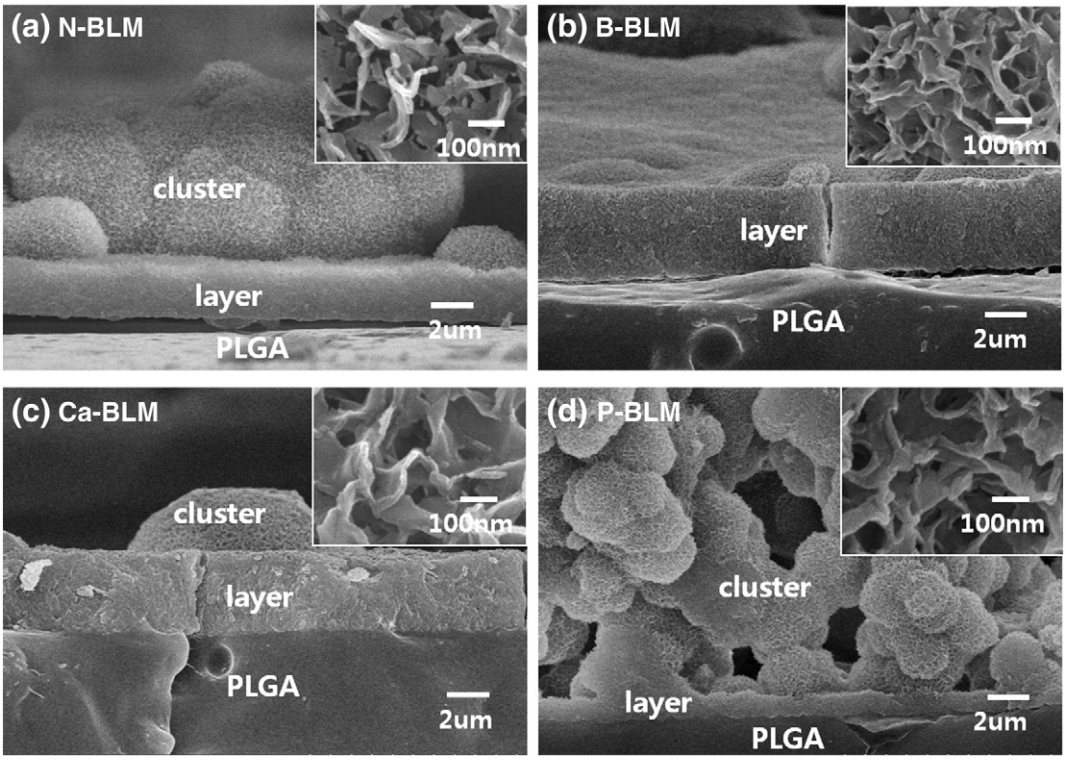

Fig. 1. Cross-sectional FE-SEM images of: (a) non-coprecipitated N-BLM group, (b) BSA-coprecipitated B-BLM, (c) Ca-BLM, and (d) P-BLM groups.

thickness under the P-mSBF conditions. These results indicate that the growth mechanisms of BLM depend on the conditions under which proteins are mixed into mSBF, resulting in differences in thickness and density of the mineral. Specifically, premixing BSA with phosphate ions results in a thinner, less organized mineral compared to premixing with calcium ions or no premixing. In magnified SEM images (Fig. 1, inset), the edges of the BLM crystals in the BSA-coprecipitated groups were more rounded compared with those of the N-BLM group, which agrees with other reports [1,5,6].

Phosphate, carbonate and amide peaks were observed via FT-IR spectroscopy (Fig. 2). The carbonate peaks (874, 1410, and 1450 cm^{-1}) showed that BLM had a carbonated apatite crystalline structure. The amide peaks (1536 and 1654 cm^{-1}) originating from BSA were observed on all 3 BSA-coprecipitated BLM groups. The intensities of the PO_4^{3-} peaks (561, 601, and 1025 cm^{-1}) of the B-BLM and Ca-BLM groups were higher than those of the control mineral and mineral created by premixing with phosphate ions. When ATR is used in FT-IR measurements, the penetration depth of IR into the sample is typically 0.5–2 μm [13]. Therefore, the density and the flatness of specimen affect the intensity of FT-IR spectra. The high intensity of FT-IR peaks of the B-BLM and Ca-BLM groups suggests that these groups have a higher density of BLM crystallites and less roughness of the BLM layer, as confirmed by SEM (Fig. 1).

The XRD patterns of all groups were assigned to a HAp structure (Fig. 3). The peak denoted as A is a combination of (211), (112), and (300) peaks, due to their wide peak widths. The intensity ratio ($I_{(002)}/I_{(A)}$) and FWHM values of the (002) peaks were calculated (Fig. 4). The mean $I_{(002)}/I_{(A)}$ value of the B-BLM group was 2-fold higher than that of the N-BLM group, and the $I_{(002)}/I_{(A)}$ of Ca-BLM was 3-fold higher and significantly greater than that of N-BLM. These results indicate that the B-BLM and Ca-BLM groups grew with a preferred orientation to the c-axis of the crystallites, and BSA affects the growth direction of BLM. On the other hand, the $I_{(002)}/I_{(A)}$ value of Ca-BLM was significantly greater than that of the P-BLM group ($p<0.05$), even though both groups were coated using a BSA-incorporated mSBF. The Ca-BLM group was coated with BSA premixed with a $CaCl_2$ solution, whereas the P-BLM group was coated with BSA premixed with a KH_2PO_4 solution. Some calcium ions were bound to BSA in Ca-mSBF, whereas phosphate ions were bound to BSA in P-mSBF before formation of BLM. The growth mechanism of BLM on PLGA could be changed by these different chemical conditions of Ca-mSBF and P-mSBF. The $I_{(002)}/I_{(A)}$ value of the B-BLM group was closer to that of the Ca-BLM group than that of P-BLM group. Therefore, the B-BLM and Ca-BLM groups were likely coated under similar chemical conditions.

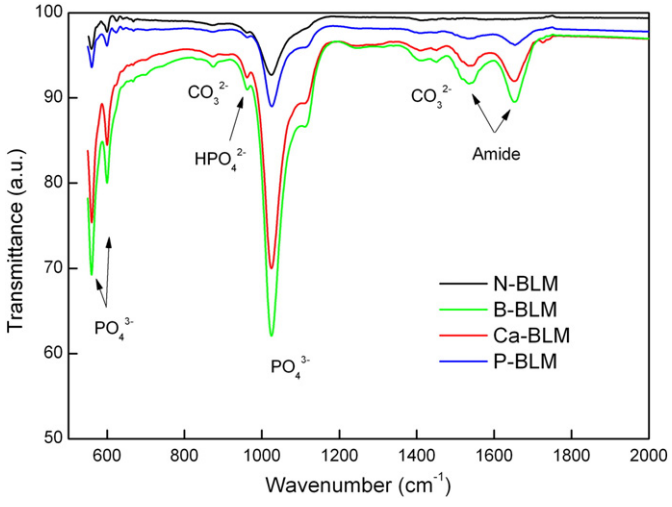

Fig. 2. FT-IR spectra of non-coprecipitated N-BLM group and BSA-coprecipitated B-BLM, Ca-BLM, and P-BLM groups measured using the ATR accessory.

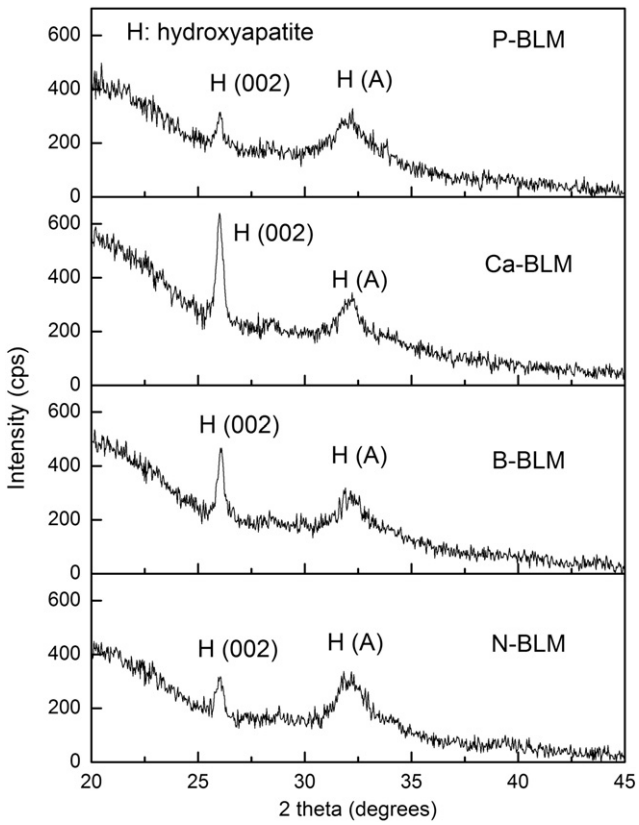

Fig. 3. X-ray diffraction patterns of the non-coprecipitated N-BLM group and BSA-coprecipitated B-BLM, Ca-BLM, and P-BLM groups. Peaks denoted as A represent a combination of (211), (112) and (300) peaks.

The FWHM values of the XRD (002) peak of the B-BLM and Ca-BLM groups were lower than that of the N-BLM group but the differences were not significant. However, the FWHM of the P-BLM group was significantly higher than that of the B-BLM and Ca-BLM groups ($p<0.05$). There was no significant difference in the FWMH of peak A in all groups. In general, a narrow XRD peak indicates high crystallinity. Therefore, the crystallinity of the c-axis of the P-BLM group was lower than that of the other groups, whereas that of the B-BLM and Ca-BLM groups did not decrease by coprecipitating BSA with BLM. The XRD patterns therefore suggest that the crystallinity of BLM is affected by the BSA mixing procedure, and this may explain contradictory trends in crystallinity when proteins are coprecipitated with BLM [1,5,8,9].

TEM images of the N-BLM, B-BLM and Ca-BLM groups (Fig. 5) show the cross-sectional structure of the BLM layers grown on PLGA relative to the SEM images (Fig. 1). The TEM image of the P-BLM group shows the cross-sectional structure of the BLM cluster coated on the BLM layer. The nano-wire shaped crystallites were caused by matching the crystalline planes of the sheet-like crystallites composing the BLM with the electron beam. The TEM images of Ca-BLM showed that these crystallites were aligned to the same direction from bottom to top, while those of the N-BLM and P-BLM groups were grown randomly. The TEM-level ultrastructure of B-BLM was more similar to Ca-BLM than to N-BLM or P-BLM. The lattice images of the BLM crystals had an HAp crystalline structure (HRTEM in inset of Fig. 5(a) and (c)). These images indicated that the (100) crystalline planes of the HAp structure were aligned to the transverse direction of the BLM crystal. These lattice planes were observed more clearly in the HRTEM image of Ca-BLM. The c-axis of the HAp structure, a hexagonal structure, is perpendicular to the a-axis ((100) crystalline plane). The XRD patterns of the Ca-BLM (Fig. 3) showed a high intensity (002) peak, which indicates that the BLMs were grown along the c-axis. Therefore, the alignment of

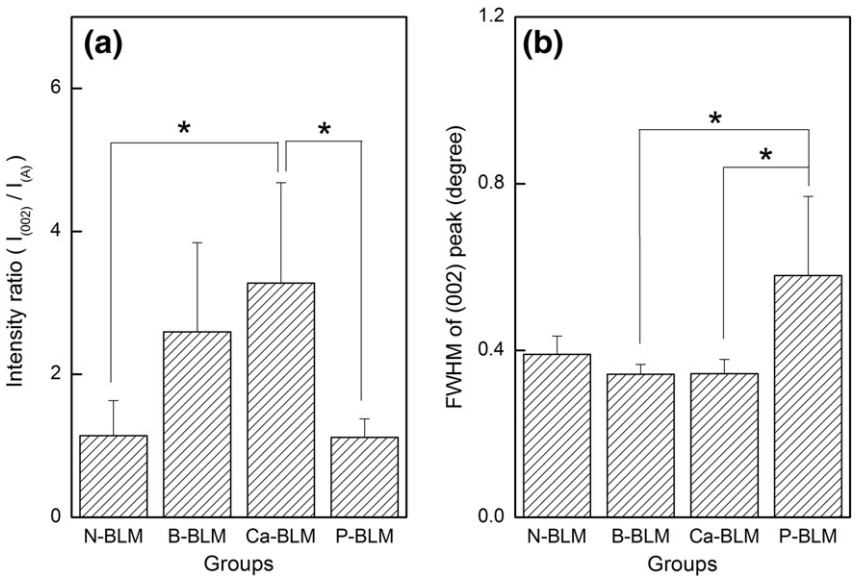

Fig. 4. (a) $I_{(002)}/I_{(A)}$ values and (b) FWHMs of (002) peaks calculated from the XRD patterns. * indicates significantly different ($p<0.05$).

crystallites shown in the TEM image of Ca-BLM (Fig. 5(b)) was due to the preferential growth of BLM to the c-axis.

Fig. 6 shows high resolution XPS spectra of C 1 s (a), N 1 s (b), Ca 2p (c) and P 2p (d). The intensity of N 1 s for N-BLM was approximately zero compared with the intensities of the coprecipitated groups because N-BLM does not contain BSA. The shape of C 1 s for N-BLM was different from those of coprecipitated groups, whereas the shape of C 1 s for the coprecipitated groups was similar to that of BSA. Therefore, it is concluded that C 1 s peaks of N-BLM originated from carbonate or another C-O functional group in mineral and C 1 s peaks of BSA-coprecipitated groups originated from BSA. For the XPS spectra of Ca and P, the peak intensities of the BSA-coprecipitated

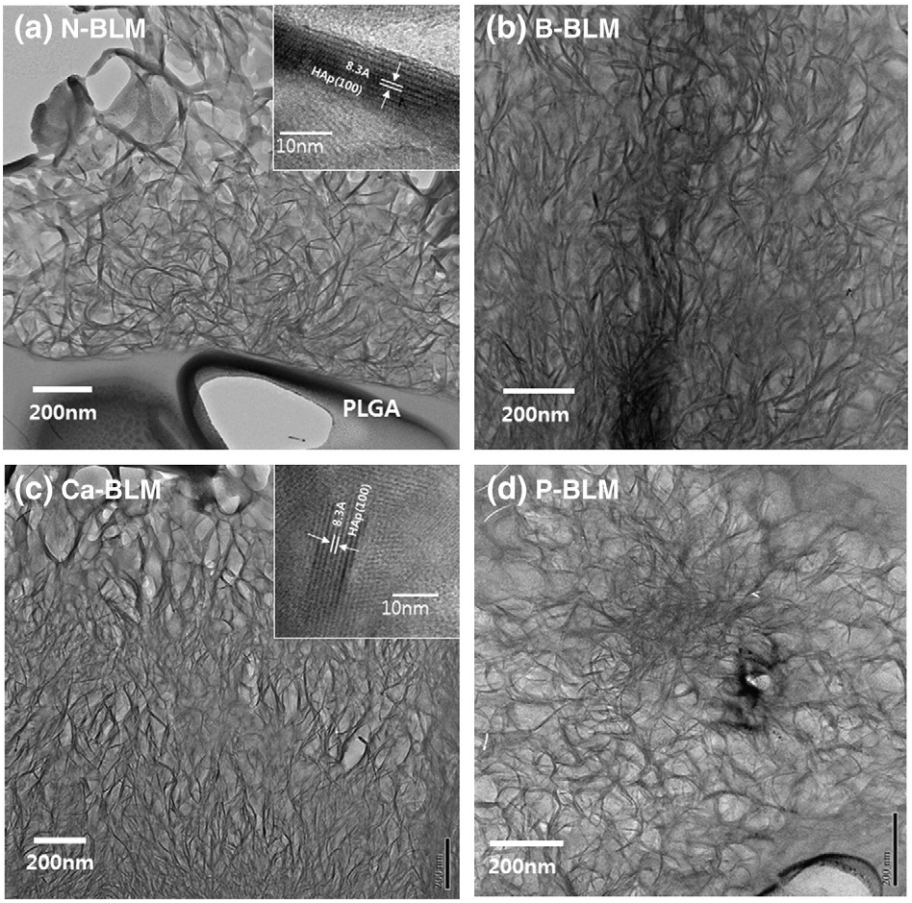

Fig. 5. TEM images of: (a) non-coprecipitated N-BLM, (b) BSA-coprecipitated B-BLM, (c) Ca-BLM and (d) P-BLM groups. HRTEM images of N-BLM and Ca-BLM are shown in the insets.

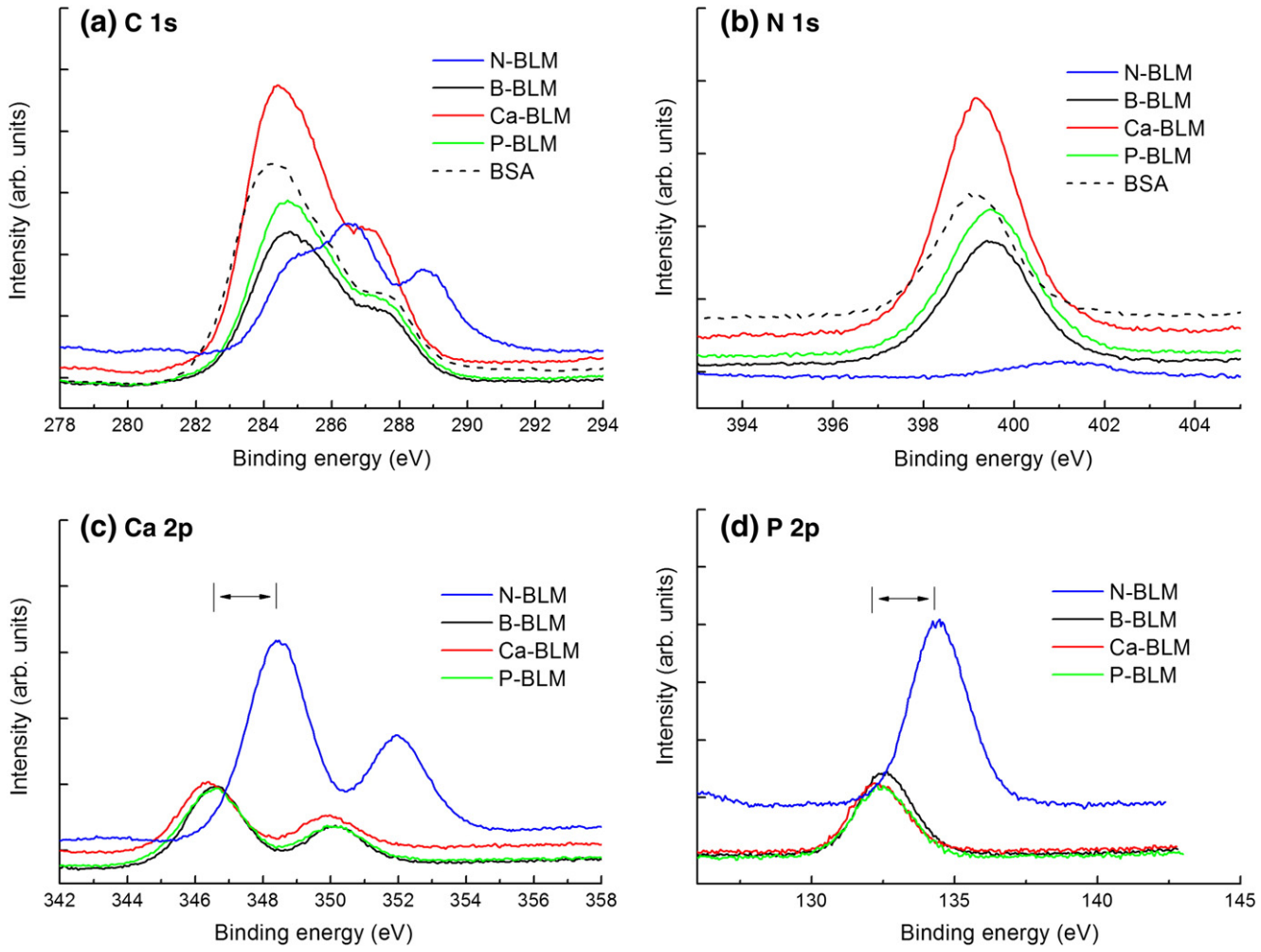

Fig. 6. High resolution XPS spectra of (a) C 1 s, (b) N 1 s, (c) Ca 2p, and (d) P 2p for non-coprecipitated N-BLM group, and BSA-coprecipitated B-BLM, Ca-BLM, and P-BLM groups. C 1 s (a) and N 1 s (b) include XPS spectrum of BSA. Arrows in (c) and (d) indicate shifts in binding energy due to co-precipitation with protein.

groups decreased and their peak energies shifted to a lower energy than that of the N-BLM group. The binding energy shift of the Ca 2p and P 2p spectra indicates that Ca or P ions are covalently or ionically bonded with a functional group of BSA in the coprecipitated specimens [14]. The XPS peak energies were similar for the Ca-BLM and P-BLM groups, even though their crystalline structures were different, as shown via XRD and TEM. The chemical conditions between BSA and inorganic ions in mSBF differed according to the BSA mixing procedure. On the other hand, XPS results indicated that the chemical binding states between BSA and BLM in the Ca-BLM and P-BLM groups were similar. Therefore, the BSA mixing procedure only affects the growth mechanism of the BLM crystallites and both calcium and phosphate ions were chemically bound with BSA in the resulting BLM.

Based on differences in BLM crystalline structure with BSA mixing procedures, growth mechanisms are inferred. When Ca-mSBF and P-mSBF were prepared, the same concentration of BSA was premixed with different amounts of $CaCl_2$ (5 mM) and KH_2PO_4 (2 mM). Therefore, it is possible that there are different amounts of bound vs. free BSA between Ca-mSBF and P-mSBF. These different concentrations of free BSA could affect the crystalline structure of BLM. However, it can be inferred that the amount of free BSA is highest in B-mSBF which was prepared before BSA mixing. On the other hand, the amount of free BSA in P-mSBF may be lower than in Ca-mSBF because the concentration of KH_2PO_4 was higher than that of $CaCl_2$. Thus, if free BSA plays a role in controlling BLM crystalline structure, then P-BLM would be more similar to B-BLM than Ca-BLM. However, P-BLM was different from B-BLM. The denaturation of BSA in $CaCl_2$ and KH_2PO_4 solutions could be a cause of the difference in BLM crystallinity. However, BSA-containing $CaCl_2$ and KH_2PO_4 solutions used in this study had pH 6.0 and 5.6, respectively. Brahma et al. [15] reported that BSAs are highly aggregated and irreversibly form a partially unfolded dimeric intermediate at a pH of 4.2, which is more acidic compared with the pH of BSA-containing $CaCl_2$ and KH_2PO_4 solutions. Therefore, it can be concluded that the chemical binding state between BSA and inorganic ions in mSBF plays the most important role in controlling BLM formation.

The following mechanism is proposed to explain the effect of protein mixing on the crystalline characteristics of BLM (Fig. 7). In HAp crystals of a hexagonal structure, calcium ions are rich on the *ac* (or *bc*) face (C-sites), parallel to c-axis, while phosphate ions or hydroxyl groups are rich on the *ab* face (P-sites), perpendicular to the c-axis [16]. This indicates that Ca ions bind to C-sites more readily, while phosphate ions bind to P-sites when HAp crystallites are grown from SBF. In Ca-mSBF, calcium ions combine with carboxyl groups (COO^-) of BSA. These calcium ions binding with BSA will be precipitated to form BLM and can be bound to C-sites more easily than P-sites. Therefore, BSA will be accumulated at C-sites and restrict the growth of *ac (or bc)* faces of HAp. It is inferred that this growth scenario controls the orientation of HAp crystallites and leads to alignment of BLM layers to the c-axis in the Ca-BLM group. However, phosphate ions combine with NH_3^+ groups in BSA when premixed within the P-mSBF group, and bind to P-sites more easily than

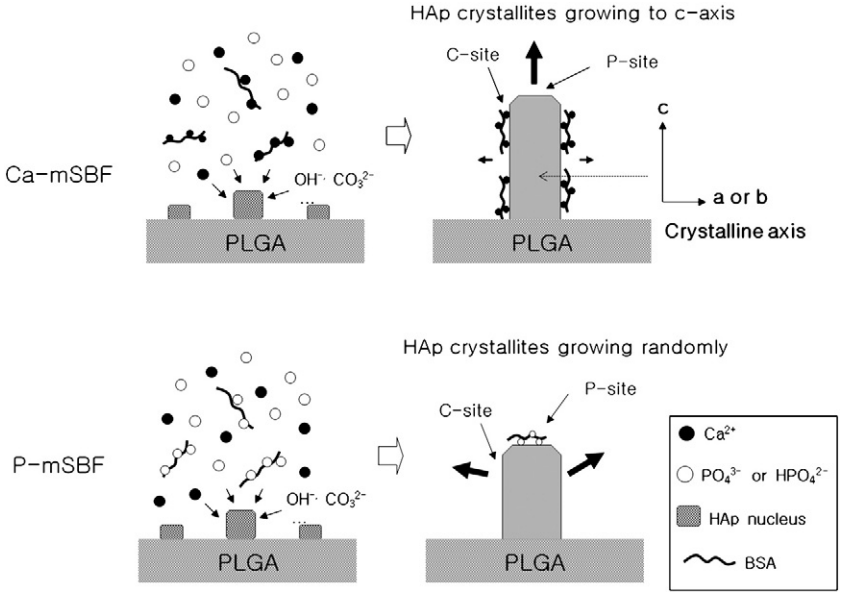

Fig. 7. Schematic demonstrating the growth of HAp crystallites in BSA-containing Ca-mSBF and P-mSBF. The HAp crystallites in Ca-mSBF are growing preferential to the c-axis, while those in P-mSBF are growing randomly.

C-sites. Therefore, a rich BSA content on an *ab* face may hinder the growth of BLM to the c-axis. The low crystallinity of the c-axis and the disordered orientation of P-BLM group, as shown via XRD and TEM, are attributed to this growth mechanism. When BSA was mixed with pre-made mSBF, BSA or its complex could bind to calcium ions in mSBF because BSA, having an isoelectric point (pI) of 4.7, is negatively charged under physiological conditions. Several studies have suggested that the carboxyl groups of BSA or collagen combine with Ca^{2+} through electrostatic interactions [10,17,18]. Therefore, the growth mechanism of B-BLM is similar to that of Ca-BLM.

The solubility of BLM coatings plays an important role in regulating the delivery of biological factors coprecipitated into BLM, because growth factors are chemically bound to the three-dimensional crystal lattice of the BLM [5]. This study showed that the crystallinity of BLM can be controlled by changing the mixing method of BSA into mSBF. The solubility of carbonated apatite increases with broadening of the (002) XRD peak, that is a decrease in crystallinity [19,20]. Therefore, P-BLM coated using P-mSBF is likely more soluble than B-BLM and Ca-BLM because P-BLM has a lower crystallinity, and BSA coprecipitated via this method is expected to be released more rapidly.

This study showed that a model protein incorporated into bone-like mineral via simple mixing or premixing with calcium ions does not result in a decrease in crystallinity, although some studies have found that BSA decreases the crystallinity of BLM [5,8,9]. The crystallinity of BLM coated using coprecipitation is affected by the chemical binding state of BSA with inorganic ions and its content in mSBF. Also, the cross-sectional SEM images (Fig. 1) did not show that BSA inhibits BLM formation. However, the change in crystallinity of BLM with BSA mixing method could be explained by BSA restricting the growth of BLM in certain orientations. Depending on the concentration of a protein in SBF, it can act as a promoter of mineralization, inhibitor or both [21]. Therefore, even though a BSA concentration of 200 g/mL did not affect BLM formation in this study, it can be inferred that BSA could act as inhibitor of BLM formation, if a high enough concentration was used for coprecipitation.

The methods of mixing BSA with mSBF could be applied to other, more biologically relevant growth factors because proteins have ionizable chemical groups such as carboxyl and amino groups. Among the growth factors with a similar pI to BSA, are acidic fibroblast growth factor (aFGF) and epidermal growth factor (EGF) which have pIs of 5.6 and 4.6, respectively. However, the effect of each protein used for coprecipitation on the crystallinity and formation rate of BLM will be different because the size, the isoelectric point, and the chemical state of proteins are different.

4. Conclusions

BSA-coprecipitated with bone-like mineral was coated onto PLGA substrates using different methods of mixing BSA with mSBF. The coprecipitated mineral formed by adding BSA directly to mSBF or premixing with $CaCl_2$ exhibited densely coated, thick BLM layers with crystallites aligned to the c-axis. In contrast, mineral formed by premixing BSA with KH_2PO_4 exhibited loosely connected BLM clusters and had a lower crystallinity. The alignment to the c-axis of Ca-BLM and the disordered orientation of P-BLM were caused by calcium ions bound to BSA in Ca-mSBF and phosphate ions bound to BSA in P-mSBF, respectively. This study showed that the crystallinity and morphology of BLM can be controlled by the mixing of BSA in mSBF, and these material characteristics of BLM could affect the controlled delivery of therapeutic molecules from BLM.

Acknowledgments

This research was supported by the Basic Science Research Program through the National Research Foundation of Korea (NRF) funded by the Ministry of Education, Science and Technology (2009–0070054, HJS) and NIH DE013380 and DE015411 (DHK).

References

[1] H.B. Wen, J.R. de Wijn, C.A. van Blitterswijk, K. de Groot, K, J. Biomed. Mater. Res. 46 (1999) 245–252.
[2] W.L. Murphy, D.H. Kohn, D.J. Mooney, J. Biomed. Mater. Res. 50 (2000) 50–58.
[3] W.L. Murphy, M.C. Peters, D.H. Kohn, D.J. Mooney, Biomaterials 21 (2000) 2521–2527.
[4] J. Morandian-Oldak, H.B. Wen, G.B. Schneider, C.M. Stanford, Periodontology 2000 (41) (2006) 157–176.
[5] L.N. Luong, S.I. Hong, R.J. Patel, M.E. Outslay, D.H. Kohn, Biomaterials 27 (2006) 1175–1186.
[6] Y. Liu, P. Layrolle, J. de Bruijn, C. van Blitterswijk, K. de Groot, J. Biomed. Mater. Res. 57 (2001) 327–335.
[7] X. Yu, H. Qu, D.A. Knecht, M. Wei, J. Mater. Sci. Mater. Med. 20 (2009) 287–294.
[8] J. Xie, C. Riley, K. Chittur, J. Biomed. Mater. Res. 57 (2001) 357–365.

[9] S.V. Dorozhkin, E.I. Dorozhkina, Colloids Surf. A 215 (2003) 191–199.
[10] Y. Wu, B. Yang, J. Lu, Z. Gu, X. Zhang, Key Eng. Mater. 330–332 (2007) 581–584.
[11] W.L. Murphy, D.J. Mooney, J. Am. Chem. Soc. 124 (2002) 1910–1917.
[12] T. Kokubo, T. Hiroaki, Biomaterials 27 (2006) 2907–2915.
[13] F.M. Mirabella Jr., in: Practical Spectroscopy Series v, Internal reflection spectroscopy theory and applications, 15, Marcel Dekker, Inc., New York, 1993, pp. 17–52.
[14] B. Feng, J. Chen, X. Zhang, Biomaterials 23 (2002) 2499–2507.
[15] A. Brahma, C. Mandal, D. Bhattacharyya, Biochim. Biophys. Acta Protein Proteomics 1751 (2005) 159–169.
[16] K. Kandori, S. Tsuyama, H. Tanaka, T. Ishikawa, Colloids Surf. B 58 (2007) 98–104.
[17] S.H. Rhee, J.D. Lee, J. Tanaka, J. Am. Ceram. Soc. 83 (2000) 2890–2892.
[18] C. Combes, C. Rey, M. Freche, J. Mater. Sci. Mater. Med. 10 (1999) 153–160.
[19] A.A. Baig, J.L. Fox, R.A. Young, Z. Wang, J. Hsu, W.I. Higuchi, A. Chhettry, H. Zhuang, M. Otsuka, Calcif. Tissue Int. 64 (1999) 437–449.
[20] D. Bayraktar, A.C. Tas, J. Eur. Ceram. Soc. 19 (1999) 2573–2579.
[21] C. Combes, C. Rey, Biomaterials 23 (2002) 2817–2823.